Fibers and Polymers 2006, Vol.7, No.2, 123-128

Modeling of Anisotropic Creep Behavior of Coated Textile Membranes

Woong-Ryeol Yu*, Min Sun Kim[1], and Joon Seok Lee[2]

School of Materials Science and Engineering, Seoul National University, Seoul 151-742, Korea
[1]Textile Research Team, Korea Institute of Industrial Technology, Cheonan 330-825, Korea
[2]School of Textiles, Yeungnam University, Gyeongsan 712-749, Korea
(Received February 24, 2006; Revised June 1, 2006; Accepted June 8, 2006)

Abstract: The present study aims at characterizing and modeling the anisotropic creep behavior of coated textile membrane, a class of flexible textile composites that are used for moderate span enclosures (roofs and air-halls). The objective is to develop a creep model for predicting the lifetime of coated textile membrane. Uniaxial creep tests were conducted on three off-axis coupon specimens to obtain the directional creep compliance. A potential with three parameters is shown to be adequate for modeling the anisotropic creep behavior of coated textile membrane. Furthermore, a possibility of predicting the creep deformation of coated textile membrane in a multi-axial stress state is discussed using the three-parameter potential.

Keywords: Creep, Anisotropy, Multi-axial stress, Textile, Coated membrane

Introduction

Coated textile membrane (CTM) forms a class of flexible textile composites that are used for moderate span enclosures (roofs and air-halls), where their properties of lightness, high tensile strength, durability and fire resistance may be exploited [1]. CTM is tensioned in the multi-axial directions to form complex shape and maintained for a considerable period. Due to the polymeric nature of the coating material (e.g., PVC) and polymeric fabric reinforcement, CTM deforms gradually in a time dependent manner at constant stress, causing them to look unfavorable and at worst to fail. Therefore, to effectively design a membrane structure, the time dependent deformation of CTM should be analyzed such that the relaxed stress can be compensated by applying tension and the excessive creep strain can be also predicted to assess the reliability of a coated textile membrane and its structure.

The salient feature of creep behavior is that strain develops at constant stress and temperature as time. Since creep brings out unfavorable dimensional change, deteriorate structural performance, and material failure at worst, many studies were performed for characterizing the viscoelastic properties of polymers [2]. Recently, for computational analysis of complex deformations, three dimensional creep behavior of solid polymer was modeled using plastic potential that can describe the isotropic deformation behavior [3,4]. These studies on the creep behavior of polymer did not consider the anisotropic behavior because a bulk polymer without reinforcement may not show significant anisotropy.

CTM has textile reinforcements made from polymeric fiber, e.g., polyester fiber. The textile reinforcement including woven, knitted, and nonwoven fabrics causes the membrane to mechanically behave in an anisotropic manner, mainly orthotropic. Some efforts have been made to characterize the creep behavior of geotextiles, which are used as the reinforcements in geotechnical and civil engineering field [5,6]. These studies focused on the characterization of long-term creep behavior of geotextiles using the accelerated creep tests at elevated temperatures and temperature-time superposition principle; however in those works the anisotropic creep behavior was not considered. Recently, an experimental study on the anisotropic creep behavior has been reported for nonwoven geotextiles [7]. Uniaxial creep test using off-axis coupon specimen was used to show the anisotropic creep behavior for the nonwoven.

As for modeling of the anisotropic creep behavior, Sun *et al.* studied the creep behavior of uniaxial fiber reinforced plastic (FRP) composites in which continuous fibers were reinforced in a direction in laminae [8-10]. FRP used for those studies were advanced structural composites using rigid fiber, e.g., graphite and carbon. Since such rigid fiber does not contribute to the creep deformation, they assumed no creep deformation in the fiber direction. They adopted a quadratic plastic potential to model the anistropic creep behavior, defining an effective stress and creep strain rate which are adequate to analyzing the creep behavior of composites in the multi-axial stress state.

The current study is concerned with modeling of the anisotropic creep behavior of CTM. While fibers in the advanced composite can be assumed to not deform due to their rigidity, polyester fibers in coated textile membrane is not as rigid as carbon or graphite, thereby they can deform time dependently under constant load at constant temperature. Therefore, a potential that can describe the creep deformation in the fiber directions is introduced to express the anisotropic creep behavior of CTM. Prior to the theoretical modeling of the anisotropic creep behavior, experimental results are first reported as follows.

Material Characterization

Off-axis Testing and Results

A basic approach used here in characterizing the anisotropic creep behavior of CTM is to conduct the uniaxial tension

*Corresponding author: woongryu@snu.ac.kr

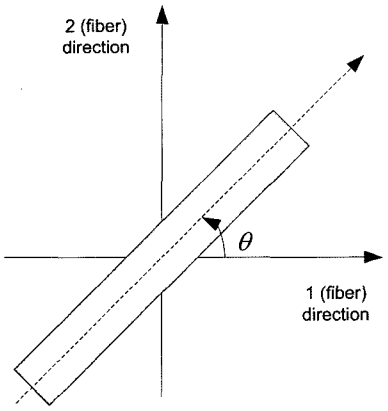

Figure 1. Schematic of off-axis coupon specimen for uniaxial creep testing.

test at constant load and an elevated temperature for a specific period. CTM used here consists of PET plain weave (28 wpi × 26 ppi) as a reinforcement and PVC for coating material. To account for the effects of anisotropy, off-axis coupon specimens with 50 mm width (and 0.67 mm thickness) were cut at angles of 0°, 45°, and 90°. Figure 1 shows a schematic of the specimen configuration used. The gage length of specimen was 150 mm for 0° specimen, 90 mm and 175 mm for 45° and 90°, respectively. The gauge length was determined considering the inside space of temperature chamber attached to a creep tester and the compliance of the specimen.

Creep tests were conducted at 60 °C for 140 hours, and 60 kg, 20 kg, and 60 kg of constant loads were applied to 0°, 45°, and 90° specimens, respectively. Only one load level for each specimen was applied to observe the anisotropic creep deformation in the current study, so that the nonlinear creep behavior is not included and will be studied in a future study. To normalize the loads applied, the creep compliance (time dependant strain divided by the nominal stress) was

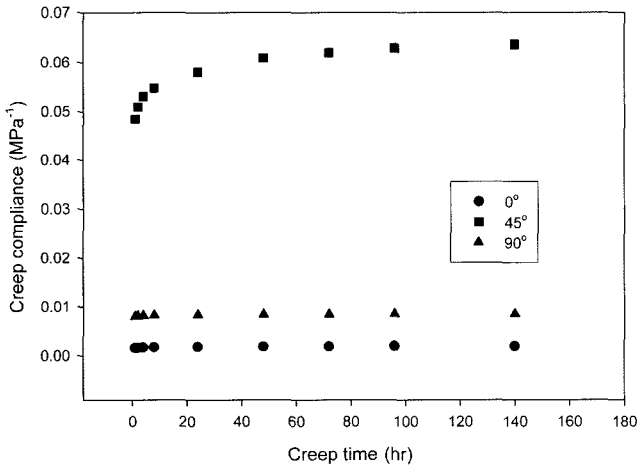

Figure 2. Creep compliance of coated textile membrane.

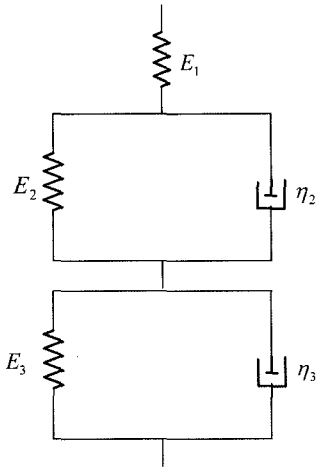

Figure 3. Five-parameter viscoelastic model.

calculated. Figure 2 shows the creep compliance curves of all the off-axis specimens for 140 hours, demonstrating that the creep behavior of coated textile membrane is significantly anisotropic depending on the fiber orientation.

A phenomenological viscoelastic model is considered to describe the creep compliance for each off-axis specimen. Five-parameter model (Figure 3), consisted of one spring element and two Voigt elements in series, was chosen such that a predicted creep compliance using the model fits the experimental one well. Using the five-parameter viscoelastic model, creep compliance ($J(t)$) was calculated through Laplace transformation of the differential equilibrium equation as follows.

$$J(t) = \frac{\varepsilon(t)}{\sigma_0} = \frac{1}{E_1} + \frac{1}{E_2}(1 - e^{-t/\lambda_2}) + \frac{1}{E_3}(1 - e^{-t/\lambda_3}) \qquad (1)$$

where $\lambda_i = \eta_i/E_i$ are retardation times, while σ_0 and $\varepsilon(t)$ are applied constant stress and time dependant strain, respectively. Nonlinear regression technique was used to determine the five parameters (E_1, E_2, E_3, λ_2, and λ_3) that fit the experimental data as possible as close (see Table 1). Figure 4 compares the compliance curves obtained through the nonlinear regression with the experimental creep compliances, showing reasonable agreement.

Creep Potential and Effective Quantities

Strain resulting from the application of a constant stress can be assumed to be decomposed into time independent initial strains and time-dependent creep strains. In the rate

Table 1. Five-parameter determined using nonlinear regression

Specimen	$1/E_1$ (MPa^{-1})	$1/E_2$ (MPa^{-1})	$1/\lambda_2$ (s^{-1})	$1/E_3$ (MPa^{-1})	$1/\lambda_3$ (s^{-1})
0°	1.558×10^{-3}	2.113×10^{-4}	0.3235	2.28×10^{-4}	0.3235
45°	4.42×10^{-2}	8.36×10^{-3}	0.6327	1.12×10^{-2}	0.0272
90°	7.87×10^{-3}	3.75×10^{-4}	0.4014	3.02×10^{-4}	0.0222

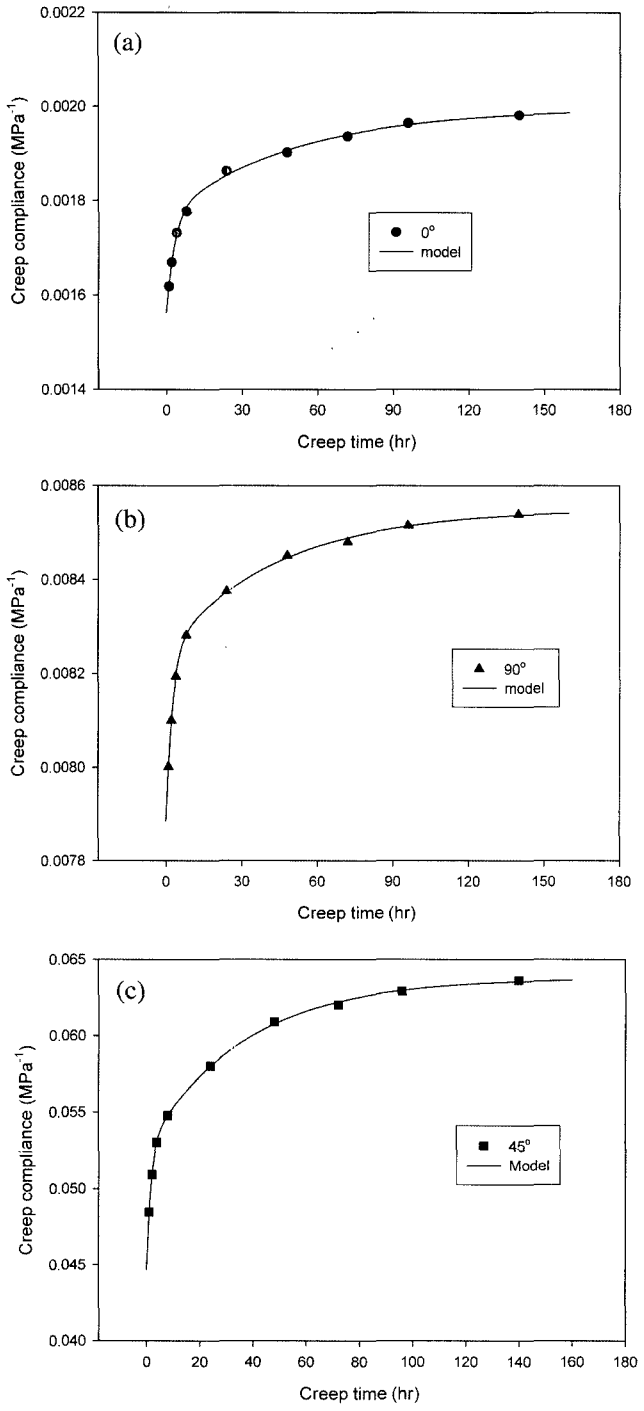

Figure 4. Fitted creep compliance using five-parameter phenomenological visco-elastic model.

formulation, total strain may be expressed for multi-axial strain state as follows.

$$\dot{\varepsilon}_{ij} = \dot{\varepsilon}^e_{ij} + \dot{\varepsilon}^c_{ij} \tag{2}$$

where the elastic strains ε^e_{ij} are assumed to occur instantaneously as the load is applied, and ε^c_{ij} are creep strains. This decomposition has been used extensively for elasto-plastic deformation analysis for which $\dot{\varepsilon}^c_{ij}$ is replaced with $\dot{\varepsilon}^p_{ij}$, and also was adopted for describing the nonlinear behavior of unidirectional fiber composite in [7] and the anisotropic creep behavior of the same material in [8]. In these studies for fibrous composites, a potential was proposed to model the creep deformation assuming that strain in the fiber direction is negligible as follows.

$$2f = \sigma^2_{22} + 2a_{66}\sigma^2_{12} \tag{3}$$

where 1 and 2 in subscript represent fiber and its transverse direction in the unidirectional fiber reinforced composites. In addition to the creep deformation, this potential was also successfully employed to describe plastic and viscoplastic behaviors of fibrous composites [11,12]. The parameter a_{66} is the only unknown orthotropy parameter to be determined experimentally. Then, the associated flow rule renders the creep constitutive equation, i.e.,

$$\dot{\varepsilon}^c_{ij} = \dot{\lambda}\frac{\partial f}{\partial \sigma_{ij}} \quad \text{or} \quad \begin{bmatrix} \dot{\varepsilon}^c_{11} \\ \dot{\varepsilon}^c_{22} \\ 2\dot{\varepsilon}^c_{12} \end{bmatrix} = \dot{\lambda}\begin{bmatrix} 0 \\ \sigma_{22} \\ 2a_{66}\sigma_{12} \end{bmatrix} \tag{4}$$

where $\dot{\lambda}$ is a proportionality factor. It is evident that according to this potential, the creep strain in the fiber direction vanishes, limiting its application to unidirectional fiber composites in which fibers are rigid enough to not deform.

In the current study, since CTM exhibits the creep deformation in the fiber and off-axis directions due to the low rigidity of polymeric fiber, a potential that can describe the creep deformation in the fiber direction is introduced as follows.

$$f = \frac{1}{2}(a_{11}\sigma^2_{11} + \sigma^2_{22} + 2a_{66}\sigma^2_{12} + 2a_{12}\sigma_{11}\sigma_{22}) \tag{5}$$

where a_{11}, a_{66} and a_{12} are unknown parameters. Then, the creep strains are determined as in equation (4),

$$\begin{bmatrix} \dot{\varepsilon}^c_{11} \\ \dot{\varepsilon}^c_{22} \\ 2\dot{\varepsilon}^c_{12} \end{bmatrix} = \dot{\lambda}\begin{bmatrix} a_{11}\sigma_{11} + a_{12}\sigma_{22} \\ \sigma_{22} + a_{12}\sigma_{11} \\ 2a_{66}\sigma_{12} \end{bmatrix} \tag{6}$$

This potential was used to model the orthotropic elastic-plastic deformation of Boron/Aluminum composite [13], benefited from the theory of plasticity for the sheet metals [14]. In the present study the same potential is used to model the anisotropic creep behavior of CTM in multi-axial stress state.

To determine the unknown parameters in equation (5), it is essential to employ the concept of effective stress and effective strain rate in a similarly way in [9,13]. The effective stress is

defined as

$$\bar{\sigma} = \sqrt{\frac{3}{2}}(a_{11}\sigma_{11}^2 + \sigma_{22}^2 + 2a_{66}\sigma_{12}^2 + 2a_{12}\sigma_{11}\sigma_{22})^{\frac{1}{2}} = \sqrt{3}f \quad (7)$$

The effective strain rate conjugate to the effective stress can be determined by introducing the rate of work done, i.e., $\dot{W}^c = \sigma_{ij}\dot{\varepsilon}_{ij}^c = \bar{\sigma}\dot{\bar{\varepsilon}}^c$

Using the flow rule and the second order of homogeneity of the creep potential, the effective strain rate is expressed by,

$$\dot{\bar{\varepsilon}}^c = \frac{2f}{\bar{\sigma}}\dot{\lambda} = \frac{2}{3}\bar{\sigma}\dot{\lambda} \quad (8)$$

Further, the explicit expression of the effective strain can be derived by deriving stresses in equation (6) in terms of strain rate and substituting them into equation (8) through equation (7) as follows.

$$\dot{\bar{\varepsilon}}^c = \sqrt{\frac{2}{3}}\frac{1}{\sqrt{a_{11}-a_{12}^2}}\left\{(\dot{\varepsilon}_{11}^c)^2 + a_{11}(\dot{\varepsilon}_{22}^c)^2 + \frac{2(a_{11}-a_{12}^2)}{a_{66}}(\dot{\varepsilon}_{12}^c)^2 - 2a_{12}(\dot{\varepsilon}_{11}^c)^2(\dot{\varepsilon}_{22}^c)^2\right\}^{1/2} \quad (9)$$

Determination of Three Parameters in Creep Potential

Now the unknown parameters (a_{11}, a_{22}, a_{12}) in the potential are determined using the uniaxial coupon creep test. First, stress in a coupon test, e.g., σ_θ is transformed to stresses in 1-2 coordinate (fiber direction) system (see Figure 1).

$$\begin{aligned}\sigma_{11} &= \sigma_\theta \cos^2\theta \\ \sigma_{22} &= \sigma_\theta \sin^2\theta \\ \sigma_{12} &= \sigma_\theta \sin\theta\cos\theta\end{aligned} \quad (10)$$

Then, the effective stress in equation (7) is simply expressed;

$$\bar{\sigma} = H(\theta)\sigma_\theta \quad (11)$$

where

$$H(\theta) = \sqrt{3/2}(a_{11}\cos^4\theta + \sin^4\theta + 2(a_{66}+a_{12})\sin^2\theta\cos^2\theta)^{1/2}$$

The effective strain is also derived for the coupon test;

$$\dot{\varepsilon}_\theta^c = \cos^2\theta(\dot{\varepsilon}_{11}^c) + \sin^2\theta(\dot{\varepsilon}_{22}^c) + \sin\theta\cos\theta(2\dot{\varepsilon}_{12}^c) \quad (12)$$

Using the flow rule in equation (6) and equation (8), the creep strain of θ specimen can be expressed by,

$$\dot{\varepsilon}_\theta^c = H^2(\theta)\dot{\lambda}\sigma_\theta, \quad \dot{\bar{\varepsilon}}^c = \dot{\varepsilon}_\theta^c/H(\theta) \quad (13)$$

Assuming proportional loading condition, the effective creep strain becomes,

$$\bar{\varepsilon}^c = \varepsilon_\theta^c/H(\theta) \quad (14)$$

Effective creep compliance is defined as in [10]

$$\bar{J} = \frac{\dot{\bar{\varepsilon}}^c}{\bar{\sigma}} = \frac{\varepsilon_\theta^c/H(\theta)}{H(\theta)\sigma_\theta} = \frac{\varepsilon_\theta^c}{\sigma_\theta}\frac{1}{H^2(\theta)} = \frac{J_\theta}{H^2(\theta)} \quad (15)$$

where J_θ is the creep compliance in θ direction, subtracted time independent compliance from total creep strain. Note that the axial creep compliance for an off-axis specimen can be represented by the effective creep compliance and with $H(\theta)$:

$$H^2(0^\circ) = \frac{3}{2}a_{11}, \quad H^2(90^\circ) = \frac{3}{2},$$

$$H^2(45^\circ) = \frac{3(a_{11}+1)}{8} + \frac{3}{4}(a_{66}+a_{12}) \quad (16)$$

By choosing proper parameters (a_{11}, a_{22}, a_{12}), the effective compliance for different off-axis specimens can be collapsed into a single master curve. Accordingly, a procedure to determine such parameters is equivalent to find the values of a_{11}, a_{22} and a_{12} that make each of the effective creep compliance for off-axis specimens collapsed onto the same curve. In the previous papers [8-12], try-and-error method was used for this, however in the current study, a systematic method is developed defining an objective function incorporated with the viscoelastic model in equation (1).

First three parameters are reduced to two by letting $a_{66}+a_{12} = \tilde{a}_{22}$. An objective function is formulated as follows.

$$\Phi(a_{11},\tilde{a}_{22}) = \sum_{t=1}^{n}\left\{\left(\frac{2J_0^t}{3a_{11}} - \frac{2J_{90}^t}{3}\right)^2 + \left(\frac{2J_{90}^t}{3} - \frac{J_{45}^t}{H^2(45^\circ)}\right)^2 + \left(\frac{J_{45}^t}{H^2(45^\circ)} - \frac{2J_0^t}{3a_{11}}\right)^2\right\} \quad (17)$$

where the superscript (t) on off-axis creep compliance (J_θ) denotes time step. Since the function above represents the quadratic sum of differences between each effective creep compliance curves for each off-axis specimen, a parameter set that minimizes the function may guarantee that all the effective creep compliance collapse on a single curve. Now the determination of the parameter is transformed to a minimization problem. The minimization of the objective function requires that the first derivatives of the function be zero, i.e.,

$$\frac{\partial\Phi}{\partial\mathbf{a}} = 0 \quad (18)$$

where vector $\mathbf{a}^T = [a_{11}, \tilde{a}_{22}]$

Equation (18) can be solved using Newton-Raphson (NR) method that requires the second derives of the objective function, the explicit expression of which is omitted for brevity. The two parameters are determined iteratively using the following procedure.

$$\mathbf{a}^{i+1} = \mathbf{a}^{i} + \Delta\mathbf{a}, \quad \Delta\mathbf{a} = -\left[\frac{\partial^2\Phi}{\partial\mathbf{a}\partial\mathbf{a}}\right]^{-1}\left[\frac{\partial\Phi}{\partial\mathbf{a}}\right] \tag{19}$$

Figure 5 shows the variation of residual (in equation (18)) as NR iteration continues. The initial guesses of 0.1 and 10 for a_{11} and $\tilde{a}_{22}$ were arbitrary chosen. In Figure 6 the effective creep compliances of off-axis specimen are plotted using the two parameters ($a_{11} = 0.6208$, $\tilde{a}_{22} = 56.8969$) determined using NR method, enabling all creep compliance curve for each off-axis specimen to be collapsed onto a single master curve. This fact demonstrates that the current method is an effective way of finding the proper values of the unknown parameters. A consideration on $\tilde{a}_{22}$ is necessary because it is a sum of two parameters, a_{66} and a_{12}. To determine each value in $\tilde{a}_{22}$, another measurement should be provided. In the present study, creep Poisson's ratio which is defined in a similar way as in [13] is used.

$$-\nu_{\theta}^{c} = \frac{d\varepsilon_{t\theta}^{c}}{d\varepsilon_{\theta}^{c}} = \frac{(a_{11}+1-2a_{66})\sin^2\theta\cos^2\theta + a_{12}(\sin^4\theta+\cos^4\theta)}{a_{11}\cos^4\theta + \sin^4\theta + 2(a_{12}+a_{66})\sin^2\theta\cos^2\theta} \tag{20}$$

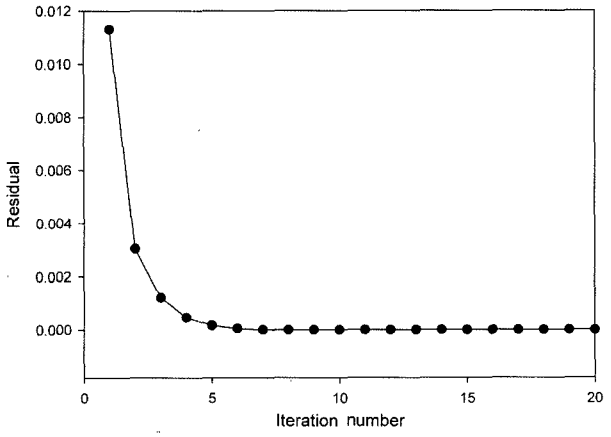

Figure 5. Minimization of the objective function by Newton-Raphson iteration.

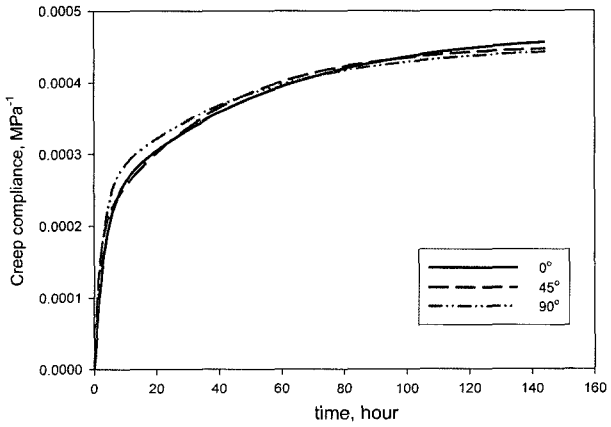

Figure 6. Effective creep compliance of each off-axis specimen ($a_{11} = 0.6208$, $\tilde{a}_{22} = 56.8969$).

where $d\varepsilon_{t\theta}^{c}$ is a strain in the transverse direction to θ direction. Taking $\theta = 0$ °, equation (20) is simplified into equation (21).

$$-\nu_{0}^{c} = \frac{a_{12}}{a_{11}} \tag{21}$$

The creep Poisson's ratio should be measured during creep testing, which may be possible by measuring the transverse strain when a constant stress is applied to 0 degree of off-axis specimen. For accurate evaluation of creep Poisson's ratio, multi-axial creep test may be more appropriate. Since a biaxial creep test machine is being built, which will make it possible to determine the creep Poisson's ratio with a reasonable accuracy, a discussion on creep Poisson's ratio will be given in a future study. If creep Poisson's ratio were determined to a value, e.g., 0.25, it would give –0.152 for a_{12} and subsequently a_{66} of 56.7417.

A Proposed Multi-axial Creep Model

A number of creep laws have been proposed for isotropic materials in various forms. These laws were generalized into the multi-axial case by replacing the uniaxial stress and strain with their effective material counter parts [13,15]. Using the effective stress and strain rate determined for CTM in the current study, a creep model can be proposed extending the uniaxial tensile test (see equation (1)) as follows.

$$\overline{\dot{\varepsilon}^{c}} = f_1(\overline{\sigma})f_2(\overline{\sigma})\exp[-f_2(\overline{\sigma})t] + f_3(\overline{\sigma})f_4(\overline{\sigma})\exp[-f_4(\overline{\sigma})t] \tag{22}$$

where f_i are unknown functions in terms of the effective stress, which can be determined by experiments. This creep model completes a constitutive model for the anisotropic creep behavior, enabling to calculate the proportional factor in equation (8) and creep strain rate in equation (6). Extensive experiments are underway to validate the current model, the result of which will be reported in a future study.

Conclusions

Anisotropic creep behavior of coated textile membrane was characterized using the uniaxial creep test of the off-axis specimen. Creep compliances in the test directions (0 °, 45 °, and 90 °) were demonstrated to be reasonably approximated by a phenomenological model (five-parameter viscoelastic model). This description plays a role to determine the orthortropic parameters for a creep potential.

To model the anisotropic creep behavior of coated textile membrane in multi-axial stress state, a three-parameter potential was introduced to describe creep strain rate using the associated flow law as in the theory of plasticity. The unknown parameters in the potential were determined using the effective creep compliance, which was defined with the effective stress and creep strain rate. As for methodology, Newton-Raphson method

was introduced to minimize an objective function that was formulated to represent the difference of the effective creep compliances for each off-axis coupon test, showing that all effective creep compliance from off-axis coupon test can collapse on a single master curve. Furthermore, a creep strain rate model for multi-axial stress case was proposed extending the result of off-axis coupon test.

Acknowledgement

This work was supported by the ERC program of MOST/ KOSEF (R11-2005-065).

References

1. J. Chilton and R. Velasco in "Design and Manufacture of Textile Composites", (A. C. Long Ed.), p.424, Woodhead Publishig Limited, Cambridge, England, 2005.
2. J. D. Ferry, "Viscoelastic Properties of Polymers", John Wiley & Sons, New York, 1980.
3. V. Kolupaev, M. Moneke, and N. Darsow, *Computational Materials Science*, **32**, 400 (2005).
4. F. Zairi, K. Woznica, M. Nait-Abdelaziz, and C. R. Mecanique, **333**, 359 (2005).
5. H. Y. Jeon, S. H. Kim, and H. K. Yoo, *Polymer Testing*, **21**, 489 (2002).
6. H.-J. Koo and Y.-K. Kim, *Polymer Testing*, **24**, 181 (2002).
7. A. Das, V. K. Kothari, A. Kumar, and M. S. Mehta, *Fibers and Polymers*, **6**(4), 313 (2005).
8. C. T. Sun and J. L. Chen, *Journal of Composite Materials*, **23**, 1009 (1989).
9. I. Chung, C. T. Sun, and I. Y. Chang, *Journal of Composite Materials*, **27**(10), 1009 (1993).
10. H. Hu and C. T. Sun, *Composites Science and Technology*, **60**, 2693 (2000).
11. C. T. Sun and I. Chung, *Composite Science and Technology*, **43**, 339 (1992).
12. S. V. Thiruppukuzhi and C. T. Sun, *Composite Science and Technology*, **61**, 1 (2001).
13. D. Kenaga, J. F. Doyle, and C. T. Sun, *Journal of Composite Materials*, **21**, 516 (1987).
14. L. M. Kachanov, "Fundamentals of the Theory of Plasticity", p.60, Mir Publishers, Moscow, 1974.
15. H. Kraus, "Creep Analysis", John Wiley & Sons, New York, 1980.